Phytochemistry Letters 27 (2018) 183–186

Contents lists available at ScienceDirect

Phytochemistry Letters

journal homepage: www.elsevier.com/locate/phytol

Anti-inflammatory terpenoid derivatives from the twigs of *Syringa oblata* var. *dilatata*

Kyoung Jin Park[a], Lalita Subedi[b,c], Sun Yeou Kim[b,c], Kang Ro Lee[a,*]

[a] Natural Products Laboratory, School of Pharmacy, Sungkyunkwan University, 2066 Seobu-ro, Jangan-gu, Suwon 16419, Gyeonggi-do, Republic of Korea
[b] Gachon Institute of Pharmaceutical Science, Gachon University, Incheon 21936, Republic of Korea
[c] College of Pharmacy, Gachon University, Incheon 21936, Republic of Korea

ARTICLE INFO

Keywords:
Syringa oblata var. *dilatata*
Oleaceae
Megastigmane
Homomonoterpenoid
Anti-inflammation

ABSTRACT

As a part of our ongoing search for bioactive constituents from Korean medicinal sources, chemical investigations of *Syringa oblata* var. *dilatata* twigs were carried out, leading to the isolation and characterization of two new terpenoid derivatives (**1**-**2**) and five known compounds (**3**-**7**). The chemical structures of the compounds **1** and **2** were determined by extensive NMR data (^{1}H and ^{13}C NMR, ^{1}H-^{1}H COSY, HSQC, HMBC, and NOESY), HRMS, and chemical methods. These compounds (**1**-**7**) were evaluated for their nitric oxide (NO) inhibitory effects in lipopolysaccharide (LPS)-activated microglial cells (BV-2). Compounds **2** and **4** exhibited significant anti-inflammatory activities, with IC_{50} values of 23.3 and 13.9 μM, respectively, which displayed similar activity to the positive control, N^{G}-monomethyl-$_{L}$-arginine ($_{L}$-NMMA, IC_{50} 20.7 μM), without any cell toxicity.

1. Introduction

Syringa oblata var. *dilatata* (Nakai) Redher (Oleacea), commonly called “Lilac”, is a deciduous shrub that grows in calcareous zones of Korea and China. It hsa been used for the treatment of vomitting, diarrhea, and rheumatalgia (Zhao et al., 2016). Several species in the *Syringa* genus have been used for the treatment of asthma, inflammation, liver, and intestinal disorders (Wang et al., 2012; Xu et al., 2010; Yin et al., 2008; Park et al., 1999). According to previous investigations on *S. oblata*, several secoiridoid glucosides, iridoids, and flavonoids with antioxidant activity have been reported (Zhao et al., 2016; Oh et al., 2003; Sun and Guo, 2013).

In a continuing search for bioactive constituents from Korean medicinal plants, we recently reported secoiridoid glucosides correlated with neuroprotective and antiproliferative activities from *S. oblata* var. *dilatata* (Park et al., 2017). In the process of finding new compounds from this plant, we further isolated two terpenoid derivatives, including a new megastigmane (**1**) and a new homomonoterpenoid (**2**), together with five known ones (**3**-**7**) from the *n*-hexane and $CHCl_3$ soluble fractions (Fig. 1). The structures of the compounds **1** and **2** were elucidated by NMR (^{1}H and ^{13}C NMR, ^{1}H-^{1}H COSY, HSQC, HMBC, and NOESY), HRMS, and chemical methods. All isolated compounds (**1**-**7**) were assessed for their effects on nitric oxide (NO) production from lipopolysaccharide (LPS)-activated BV-2 cells. Herein, we report the isolation and structural elucidation of compounds **1**-**7** and their inhibition activity of NO generation.

2. Results and discussion

The MeOH extract of *S. oblata* var. *dilatata* twigs was subjected to liquid–liquid solvent-partitioning to yield *n*-hexane, $CHCl_3$, EtOAc, and *n*-BuOH soluble fractions. Each fraction was assessed for its inhibitory effect on nitric oxide (NO) production in lipopolysaccharide-activated murine microglial cells. It was found that the *n*-hexane and $CHCl_3$ soluble fractions showed anti-inflammatory activities, with IC_{50} values of 42.4 and 29.4 μM, respectively, while the EtOAc and n-BuOH soluble fractions exhibited weak activities (72.9 and 500.1 μM, respectively). Therefore, the active *n*-hexane and $CHCl_3$ soluble fractions were investigated and resulted in the isolation of a new megastigamane (**1**) and a new homomonoterpenoid (**2**), together with five known compounds (**3**-**7**) (Fig.1).

Compound **1** was purified as a colorless gum and its molecular formula was confirmed as $C_{13}H_{20}O_4$ based on its molecular ion peak $[M + Na]^+$ at *m/z* 263.1264 (calcd for $C_{13}H_{20}O_4Na$, 263.1259) in the positive-ion HRESIMS. The UV and IR spectra showed absorption bands associated with hydroxy and α, β-unsaturated carbonyl groups (Fig. S2,S3). The ^{1}H NMR spectrum of **1** displayed signals for an olefinic proton [δ_H 5.90 (1H, s, H-1)], an oxymethine proton [δ_H 4.28 (1H, m, H-4′)], and four methyl groups [δ_H 2.26 (3H, s, H-4), 1.45 (6H, s, H-7′ and 9′), 1.22 (3H, s, H-8′)]. The ^{13}C NMR spectrum exhibited 13

* Corresponding author.
E-mail address: krlee@skku.edu (K.R. Lee).

https://doi.org/10.1016/j.phytol.2018.07.009
Received 23 May 2018; Received in revised form 21 June 2018; Accepted 12 July 2018

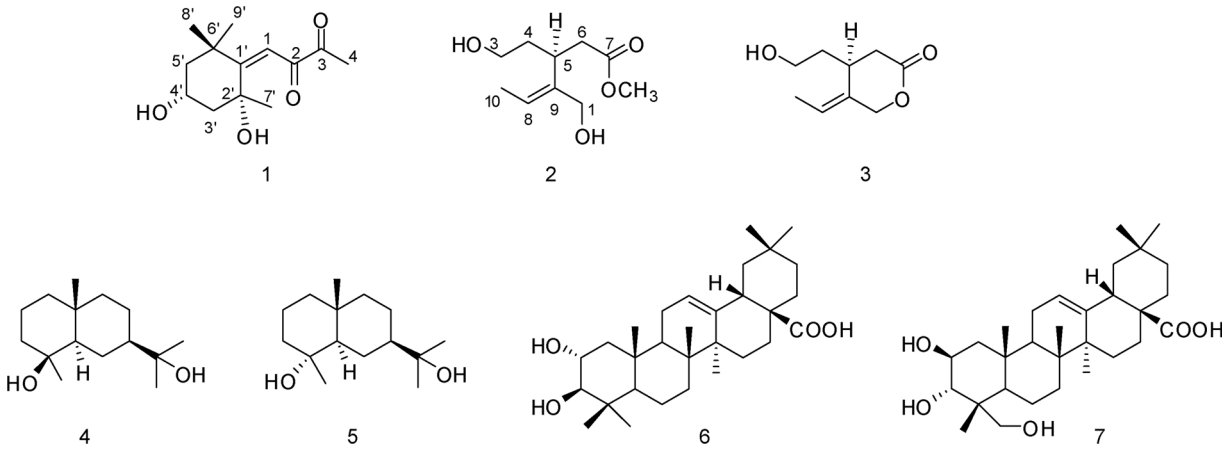

Fig. 1. Chemical structures of compounds **1**-**7**.

Table 1
^{1}H [ppm, mult., (*J* in Hz)] and ^{13}C NMR spectroscopic data of compounds **1** and **2** in Methanol-d_4.

Position	1[a]		2[b]	
	δC	δH	δC	δH
1	101.2	5.90, s	64.7	4.00, brd (2.3)
2	211.6			
3	200.9		61.2	3.51, m
4	26.6	2.26, s	37.1	1.73, m
5			33.6	3.27, m
6			39.9	2.50, dd (7.8, 3.1)
7			175.1	
8			125.1	5.64, q (6.9)
9			140.8	
10			13.4	1.67, dt (6.9, 1.1)
1′	120.1			
2′	72.5			
3′	49.9	2.26, overlap 1.45, overlap		
4′	64.5	4.28, m		
5′	50.1	2.00, brd (12.0) 14.0, brd (12.0)		
6′	37.1			
7′	30.9	1.45, s		
8′	32.4	1.22, s		
9′	29.4	1.45, s		
OCH_3			52.1	3.62, s

[a] Recorded at 700 (δH) and 175 (δC) MHz.
[b] Recorded at 500 (δH) and 125 (δC) MHz.

resonances characteristic for two carbonyl carbons (δ_C 211.6 and 200.9), two olefinic carbons (δ_C 120.1 and 101.2), an oxygenated tertiary carbon (δ_C 72.5), an oxymethine carbon (δ_C 64.5), two methine

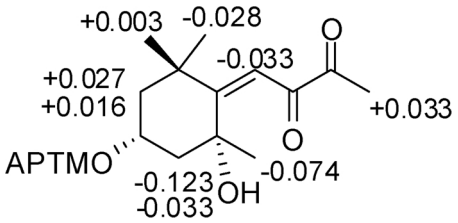

Fig. 3. Δδ values (δ_S-δ_R) in ppm of the MTPA ester derived from **1**.

carbons (δ_C 50.1 and 49.9), a quaternary carbon (δ_C 37.1), and four methyl carbons (δ_C 32.4, 30.9, 29.4, and 26.6). These spectroscopic data (Table 1) were similar to those of cannabiside D (Wu et al., 2006), except for the absence of the glucopyranose signals (see above). The planar structure of **1** was established through 2D NMR analysis, including ^{1}H–^{1}H COSY, HSQC, and HMBC spectra (Fig. 2). The HMBC cross-peak from H-1 to C-2 and from H-4 to C-3 confirmed the positions of the two carbonyl groups at C-2 and C-3, respectively (Fig. 2). The relative configuration of **1** was deduced by analyzing the NOESY data. In the NOESY spectrum (Fig. 2), strong and weak correlations of H-4′/H-5′a, H-4′/H-7′, H-5′/H-9′ were observed, which indicated H-4′ and CH_3-7′ are cofacial. The absolute configuration of C-4′ was determined by the modified Mosher's method (Kim et al., 2011). Treatment of **1** with (*R*)- and (*S*)-MTPA-Cl gave the (*S*)- and (*R*)-MTPA esters 1 s and 1 r, respectively. The assigned ^{1}H NMR signals of the two MTPA esters were calculated as the Δδ values (δ_S-δ_R) (Fig. 3). The results indicated that the absolute configuration is 4′*R*. Therefore, compound **1** was elucidated as shown in Fig. 1, and named dilatanone (**1**).

Compound **2** was isolated as a colorless gum. The molecular formula was established as $C_{10}H_{18}O_4$ from the $[M + Na]^+$ ion peak at *m/z* 225.1109 (calcd for $C_{10}H_{18}O_4Na$, 225.1103) in the positive-ion

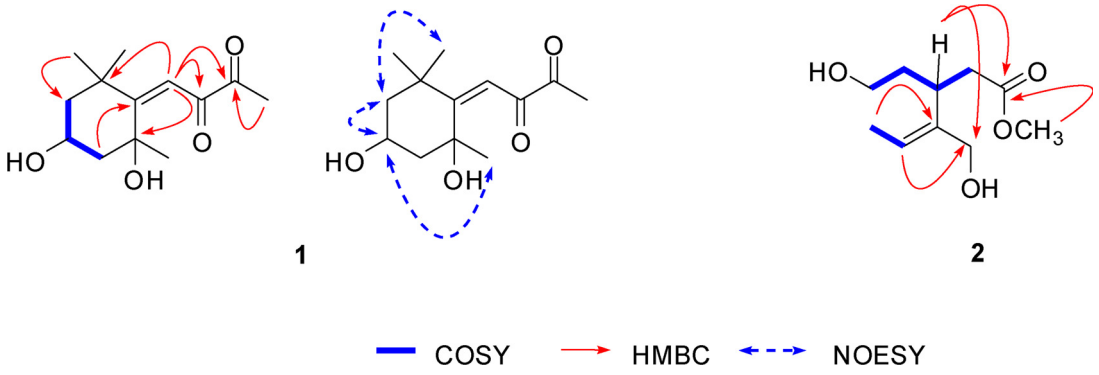

Fig. 2. Key ^{1}H-^{1}H COSY, HMBC, and NOESY correlations of **1** and **2**.

HRESIMS. The ^{1}H NMR spectrum of **2** exhibited the presence of an olefinic proton [δ_H 5.64 (1H, q, J = 6.9 Hz, H-8)], two oxymethylenes [δ_H 4.00 (2H, brd, J = 2.3 Hz, H-1) and 3.51 (2H, m, H-3)], a methine proton [δ_H 3.27 (1H, m, H-5)], two methylene protons [δ_H 2.50 (2H, dd, J = 7.8 3.1 Hz, H-6), 1.73 (2H, m, H-4)], a methyl group [δ_H 1.67 (3H, dt, J = 6.9, 1.1 Hz, H-10)], and a methoxy group [δ_H 3.62 (3H, s, $COOCH_3$)]. The ^{13}C NMR spectrum of **2** displayed 10 carbon signals including an ester carbonoyl carbon (δ_C 175.1), two olefinic carbons (δ_C 140.8 and 125.1), two oxymethylene carbons (δ_C 64.7 and 61.2), two methylene carbons (δ_C 39.9 and 37.1), a methine carbon (δ_C 33.6), a methyl carbon (δ_C 13.4), and a methoxy carbon (δ_C 52.1). The gross structure of **2** was established by analysis of the 2D NMR data (^{1}H–^{1}H COSY, HSQC, and HMBC) (Fig. 2). The location of the methoxy group was determined to be C-7 through the HMBC cross-peak between 7 − OCH_3/C-7 (Fig. 2). The absolute configuration of nocellaralactone (**3**) has been deduced through biosynthetic pathway in previous studies (Serrilli et al., 2013; Mousouri et al., 2014). The similarities of the ^{1}H and ^{13}C NMR chemical shifts at C-5 between compound **2** and nocellaralactone (**3**) imply that both possess 5*S* configuration (Table 1). Thus, the structure of **2** was determined as shown in Fig. 1, and named dilationate (**2**). Compound **2** was to be formed by methanolysis of the lactone ring of nocellaralactone (**3**).

The known compounds were identified as megaritolactonol (**3**) (Mousouri et al., 2014), 4-*epi*-cryptomeridiol (**4**) (Ando et al., 1994), cryptomeridiol (**5**) (Ando et al., 1994), maslinic acid (**6**) (Rudiyansyah and Garson, 2006), and arjunolic acid (**7**) (Rudiyansyah and Garson, 2006) by comparison of their spectroscopic data with the reported data in the references.

The anti-inflammatory effects of the isolates (**1**-**7**) were evaluated through the measurement of NO production levels in the LPS-stimulated murine microglia BV-2 cells (Table 2). Compound **4** exhibited significant inhibitory effect on NO production, with an IC_{50} value of 13.9 μM, showing higher activity than the positive control, N^G-monomethyl-$_L$-arginine ($_L$-NMMA, IC_{50} 20.7 μM), without substantial cell toxicity. Although compounds **6** and **7** also showed strong inhibitory activity (IC_{50} value of 6.2 and 6.5 μM, respectively), they reduced the cell viability of BV-2 cells (46.7 ± 0.2% and 57.6 ± 5.2%). Also compounds **2** and **3** were structually similar, but compound **2** (IC_{50} value of 23.3 μM) displayed higher inhibitory activity than compound **3** (IC_{50} value of 42.4 μM).

3. Experimental

3.1. General experimental procedures

Optical rotations were measured on a JASCO P-1020 polarimeter (JASCO, Easton, MD, USA). Infrared (IR) spectra were recorded on a Bruker IFS-66/S Fourier-transform IR spectrometer (Bruker, Karlsruhe, Germany). Ultraviolet (UV) spectra were recorded with a Shimadzu UV-1601 UV–vis spectrometer (Shimadzu, Tokyo, Japan). NMR spectra were recorded on a Varian Unity INOVA 500 NMR spectrometer (Varian Palo Alto, CA, USA) operating at 500 MHz (^{1}H) and 125 MHz (^{13}C) and a Bruker AVANCE III 700 NMR spectrometer operating at 700 MHz (^{1}H) and 175 MHz (^{13}C) with chemical shifts given in ppm (δ). HRESI mass spectra were obtained on a Waters SYNAPT G2 Q-TOF mass spectrometer (Waters, MA, USA). Preparative HPLC was performed using a Gilson 306 pump (Middleton, WI, USA) with a Shodex Refractive Index Detector (New York, NY, USA) and a Phenomenex Luna 10 μm column (250 × 10 mm) (Phenomenex, Torrance, CA, USA). Silica gel 60 (Merck, Darmstadt, 70–230 mesh, and 230–400 mesh; Merck, Darmstadt, Germany) and RP-C_{18} silica gel (Merck, 230–400 mesh) were used for column chromatography. LPLC was performed over a LiChroprep Lobar-A RP-C_{18} column (Merck, 240 mm × 10 mm i.d.) equipped with a FMI QSY-0 pump. Thin-layer chromatography (TLC) was performed using Merck pre-coated silica gel F_{254} plates and RP-18 F_{254s} plates (Merck). Spots were detected on TLC under UV light or by heating after spraying the samples with anisaldehyde-sulfuric acid.

Table 2
Inhibitory effects of compounds **1**-**7** on NO production in LPS-activated BV-2 cells.

Compound	IC_{50} (μM)[a]	Cell viability (%)[b]
1	45.9	110.8 ± 2.9
2	23.3	130.2 ± 7.4
3	42.4	112.0 ± 3.1
4	13.9	118.1 ± 6.8
5	34.9	103.6 ± 2.6
6	6.2	46.7 ± 0.2
7	6.5	57.6 ± 5.2
$_L$-NMMA[c]	20.7	101.5 ± 5.7

[a] IC50 value of each compound was defined as the concentration (μM) that caused 50% inhibition of NO production in LPS-activated BV-2 cells.
[b] Cell viability following treatment with 20 μM of each compound was determined using the MTT assay and is expressed as a percentage (%). Data are expressed as the mean ± SD of three independent experiments.
[c] Positive control.

3.2. Plant material

The twigs of *S. oblata* var. *dilatata* were collected at Suwon, Korea in June 2014. The plant was identified by one of the authors (K.R.Lee). A voucher specimen (SKKU-NPL 1404) was deposited in the herbarium of the School of Pharmacy, Sungkyunkwan University, Suwon, Republic of Korea.

3.3. Extraction and isolation

Twigs of *S. oblata* var. *dilatata* (6.9 kg) were extracted three times using 80% aqueous MeOH for 1 day under reflux, and were then filtered. The resultant MeOH extract (450 g) was suspended in distilled water (2.4 L) and then successively partitioned with *n*-hexane, $CHCl_3$, EtOAc and *n*-BuOH, yielding 15, 25, 48, and 213 g, respectively. The *n*-hexane-soluble fraction (15 g) was separated over a silica gel column (*n*-Hexane – EtOAc, 8:1 → 1:1) to yield seven fractions (H1 – H7). Fraction H6 (0.7 g) was chromatographed on an RP-C_{18} silica gel column with 60% aqueous MeOH to give 14 subfractions (H61 – H614). Fraction H65 (19 mg) was purified by semi-preparative HPLC (80% aqueous MeOH, flow rate of 2.0 ml/min) to acquire compound **4** (7 mg). Fraction H7 (0.6 g) was fractionated into 12 subfractions (H71 – D712) using an RP-C_{18} silica gel open column eluting with 60% aqueous MeOH. Compound **5** (21 mg) was obtained by purifying fraction H72 (41 mg) using semi-preparative HPLC (55% aqueous CH_3CN, flow rate of 2.0 ml/min). Fraction H75 (20 mg) was purified by semi-preparative HPLC (75% aqueous CH_3CN, flow rate of 2.0 ml/min) to yield compound **6** (8 mg). The $CHCl_3$-soluble fraction (25 g) was chromatographed on a silica gel column ($CHCl_3$ – MeOH, 60:1 → 1:1). Ten fractions (C1 – C10) were collected after TLC analysis. Fraction C6 (2.0 g) was separated on an RP-C_{18} silica gel open column, eluted with a gradient solvent system of 50 → 80% aqueous MeOH, to give six subfractions (C61 – C66). Compounds **2** (6 mg) and **3** (9 mg) were afforded from fraction C61 (239 mg) using a Lobar-A RP-C_{18} column (40% aqueous MeOH) followed by semi-preparative HPLC (22% aqueous CH_3CN, flow rate of 2.0 ml/min). Fraction C72 (200 mg) was separated by a Lobar-A RP-C_{18} column with 40% aqueous MeOH and further purified by semi-preparative HPLC (23% aqueous CH_3CN, flow rate of 2.0 ml/min) to yield compound **1** (4 mg). Fraction C8 (3.0 g) was chromatographed on an RP-C_{18} silica gel open column with 50% aqueous MeOH to give eight subfractions (C81 – C88). Fraction C88 (426 mg) was purified by semi-preparative HPLC (50% aqueous CH_3CN, flow rate of 2.0 ml/min) to acquire compound **7** (14 mg).

3.3.1. Dilatanone (1)

Colorless amorphous gum; [α]–73.3 (*c* 0.03, MeOH); IR (KBr) ν_{max} cm^{-1}: 3398, 3225, 1664; UV (MeOH) λ_{max} (log ε) 202 (0.9), 231 (0.7) nm; ^{1}H (700 MHz, CD_3OD) and ^{13}C (175 MHz, CD_3OD) NMR data, see Table 1; HR-ESI-MS (positive-ion mode) *m/z* 225.1109 [M + Na]$^+$ (calcd. for $C_{10}H_{18}O_4Na$, 225.1103).

3.3.2. Dilationate (2)

Colorless amorphous gum; [α]–2.5 (*c* 0.04, MeOH); IR (KBr) ν_{max} cm^{-1}: 3367, 2945, 2831, 1453, 1032; UV (MeOH) λ_{max} (log ε) 202 (1.1); ^{1}H (500 MHz, CD_3OD) and ^{13}C (125 MHz, CD_3OD) NMR data, see Table 1; HR-ESI-MS (positive-ion mode) *m/z* 263.1264 [M + Na]$^+$ (calcd. for $C_{13}H_{20}O_4Na$, 263.1259).

*3.4. Preparation of Mosher ester derivatives **1r** and **1s***

Compound **1** (0.5 mg) in deuterated pyridine (0.6 ml) was transferred to a clean NMR tube. (*S*)-(+)-α-Methoxy-α-(trifluoromethyl) phenylacetyl (MTPA) chloride (10 μL) (Sigma, St. Louis, MO) was added immediately into the NMR tube under a N_2 gas stream. The NMR tube was then shaken carefully to mix the sample and the MTPA chloride evenly. The NMR reaction tube was left at room temperature overnight. The reaction was then completed to afford the (*R*)-MTPA ester derivative (**1r**) of **1**. The (*S*)-MTPA ester derivative of **1** (**1s**) was obtained in the same method as **1r**. The ^{1}H NMR spectra of **1r** and **1s** were measured directly in the NMR reaction tubes.

3.4.1. 1-(R)-MTPA ester (1r)

^{1}H NMR (pyridine-d_5, 700 MHz) δ_H 6.179 (1H, m, H-4′), 5.944 (1H, s, H-1), 2.714 (1H, m, H-3′a), 2.252 (1H, m, H-5′a), 2.222 (1H, m, H-3′b), 1.828 (1H, m, H-5′b), 1.811 (3H, s, H-4), 1.629 (3H, s, H-9′), 1.575 (3H, s, H-7′), 1.130 (3H, s, H-8′).

3.4.2. 1-(S)-MTPA ester (1s)

^{1}H NMR (pyridine-d_5, 700 MHz) δ_H 6.143 (1H, m, H-4′), 5.911 (1H, s, H-1), 2.591 (1H, m, H-3′a), 2.279 (1H, m, H-5′a), 2.189 (1H, m, H-3′b), 1.844 (1H, overlap, H-5′b), 1.844 (3H, s, H-4), 1.601 (3H, s, H-9′), 1.501 (3H, s, H-7′), 1.133 (3H, s, H-8′).

3.5. Assessment of NO production and cell viability

BV-2 cells, originally developed by Dr. V. Bocchini at the University of Perugia (Perugia, Italy), were used for this study. The cells were seeded into a 96-well plate at 4×10^4 cells/well and treated with/without the purified compounds at different concentrations. LPS (100 ng/ml) was added to BV-2 cells and grown for 1d. The produced levels of nitrile (NO_2), a soluble oxidized product of NO, were evaluated with the Griess reagent (1% sulfanilamide and 0.1% *N*-1-napthylethylenediamine dihydrochloride in 5% phosphoric acid). The supernatant (50 μL) was harvested and mixed with an equal volume of Griess reagent. After 10 min the absorbance was gauged at wavelength 570 nm. Cell viability was measured using the MTT assay. N^G-monomethyl-L-arginine (NMMA, Sigma, St. Louis, USA), a well-known NO synthase inhibitor, was tested as a positive control.

4. Conclusions

In this study, seven chemical constituents, including two new compounds (**1-2**), were isolated and characterized from the twigs of *S. oblata* var. *dilatata*. The chemical structures of the compounds (**1-2**) were determined through NMR (^{1}H and ^{13}C NMR, COSY, HSQC, and HMBC), HRMS, and chemical methods. All isolated compounds (**1-7**) were evaluated for their anti-inflammatory activities. Of them, compounds **6** and **7** exhibited strong anti-inflammatory activities, but the cell viability was relatively diminished. Compounds **2** and **4** showed significant inhibition on NO production in the LPS-stimulated murine microglia BV-2 cells. Although the compound **2** could be formed during MeOH extraction, but this compound might play an important role in the anti-inflammatory acitivity of the MeOH extract of *S. oblata* var. *dilatata* twigs. The other compounds displayed moderate activities. These results indicate that *S. oblata* var. *dilatata* and its active constituents might be a potentially valuable source for new anti-neuroinflammatory agents.

Acknowledgements

This research was supported by the Basic Science Research Program through the National Research Foundation of Korea (NRF), funded by the Ministry of Education, Science and Technology (2016R1A2B2008380). We are thankful to the Korea Basic Science Institute (KBSI) for the measurements on the NMR and mass spectra.

References

Ando, M., Arai, K., Kikuchi, K., Isogai, K., 1994. Synthetic studies of sesquiterpenes with a cis-fused decalin system, 4. Synthesis of (+)-5βH-eudesma-3,11-diene, (-)-5βH-eudesmane-4β,11-diol, and (+)-5βH-eudesman-4α,11-diol, and structure revision of a natural eudesman-4,11-diol isolated from *Pluchea argute*. J. Nat. Prod. 57, 1189–1199.

Kim, K.H., Choi, S.U., Kim, Y.C., Lee, K.R., 2011. Tirucallane triterpenoids from Cornus walteri. J. Nat. Prod. 74, 54–59.

Mousouri, E., Melliou, E., Magiatis, P., 2014. Isolation of megaritolactones and other bioactive metabolites from' Megaritiki' table olives and debittering water. J. Agric. Food Chem. 62, 660–667.

Oh, H., Ko, E.K., Kim, D.H., Jang, K.K., Park, S.E., Lee, H.S., Kim, Y.C., 2003. Secoiridoid glucosides with free radical scavenging activity from the leaves of *Syringa dilatata*. Phytother. Res. 17, 417–419.

Park, H.J., Lee, M.S., Lee, K.T., Sohn, I.C., Han, Y.N., Miyamoto, K.I., 1999. Studies on constituents with cytotoxic activity from the stem bark of Syringa velutina. Chem. Pharm. Bull. 47, 1029–1031.

Park, K.J., Suh, W.S., Subedi, L., Kim, S.Y., Choi, S.U., Lee, K.R., 2017. Secoiridoid glucosides from the twigs of *Syringa oblarata* var. *dilatata* and their neuroprotective and cytotoxic activities. Chem. Pharm. Bull. 65, 359–364.

Rudiyansyah, Garson, M.J., 2006. Secondary metabolites from the wood bark of *Durio zibethinus* and *Durio kutejensis*. J. Nat. Prod. 69, 1218–1221.

Serrilli, A.M., Frasca, G., Rizza, L., Bonina, F.P., Bianco, A., 2013. Nocellaralactone, a new monoterpenoid with anti-inflammatory activity, from *Olea europaea* L., cultivar Nocellara del Belice. Nat. Prod. Res. 27, 2311–2319.

Sun, Q., Guo, Y.X., 2013. Extraction of total flavonoids from leaves of *Syringa oblata* Lindl. and numerical simulation. Zhongguo Yiyuan Yaoxue Zazhi 33, 1145–1149.

Wang, Q.H., Ao, W.L.J., Wu, Q., Ying, X., 2012. Two new neolignans from the stems of *Syringa pinnatifolia* Hemsl. var. *alashanensis*. Helv. Chim. Acta 95, 1680–1685.

Wu, B., Lin, W.H., Gao, H.Y., Zheng, L., Wu, L.J., Kim, C.S., 2006. Four antibacterial monoterpenoid derivatives from the herba of *Senecio cannabifolius* less. Indian J. Pharm. Sci. 68, 332–336.

Xu, Q.M., Li, Q., Liu, Y.L., Feng, Y.L., Yang, S.L., Li, X.R., 2010. New lignans from *Syringa reticulata* var. *mandshurica*. Chem. Nat. Compd. 46, 366–369.

Yin, W.P., Zhao, T.Z., Zhang, H.Y., 2008. A novel oligosaccharide ester from Syringa pubescens. J. Asian Nat. Prod. Res. 10, 95–100.

Zhao, M., Tang, W.X., Li, J., Bai, L.M., Wang, J.L., Zhang, W.Z., Zhang, S.J., 2016. Two new monoterpenoids from the fresh leaves of Syringa oblata. Chem. Nat. Compd. 52, 1023–1025.